Hindawi
Journal of Spectroscopy
Volume 2018, Article ID 4193657, 10 pages
https://doi.org/10.1155/2018/4193657

Research Article

Electronic Spectra of *ortho*-Substituted Phenols: An Experimental and DFT Study

Samuel Tetteh,[1] **Ruphino Zugle**,[1] **John Prosper Kwaku Adotey**,[1] **and Andrews Quashie**[2]

[1]*Chemistry Department, School of Physical Sciences, College of Agriculture and Natural Sciences, University of Cape Coast, Cape Coast, Ghana*
[2]*Institute of Industrial Research, Council for Scientific and Industrial Research, Cape Coast, Ghana*

Correspondence should be addressed to Samuel Tetteh; stoshgh2001@yahoo.com

Received 25 May 2018; Revised 21 September 2018; Accepted 25 September 2018; Published 9 October 2018

Academic Editor: Pedro D. Vaz

The electronic spectra of phenol, 2-chlorophenol, 2-aminophenol, and 2-nitrophenol have been studied both experimentally and computationally. The effect of the substituents on the solvatochromic behavior of the phenols were investigated in polar protic (methanol) and aprotic (dimethyl sulfoxide (DMSO)) solvents. The spectra of 2-nitrophenol recorded the highest red shift in methanol. The observed spectral changes were investigated computationally by means of density functional theory (DFT) methods. The gas phase compounds were fully optimized using B3LYP functionals with 6-31++G(d,p) bases set. The effects of the substituents on the electron distribution in the σ-bonds as well as the natural charge on the constituent atoms were analyzed by natural bond orbital (NBO) and natural population analysis (NPA). Second-order perturbation analyses also revealed substantial delocalization of nonbonding electrons on the substituents onto the phenyl ring, thereby increasing its electron density. Full interaction map (FIM) also showed regions of varying propensities for hydrogen and halogen bonding interactions on the phenols.

1. Introduction

The acidity and electronic properties of substituted phenols have been the subject of much research both experimentally and theoretically [1–7]. This is due to the important (bio) chemical and industrial applications of phenolic compound. They are used as starting materials in the syntheses of dyes [8, 9], manufacture of drugs [10], and disinfectants [11] as well as the study of tyrosine-containing proteins and lignin polymers [2]. Polyphenols have been well investigated as antioxidants because the phenolic hydrogen can easily be donated to quench the activity of free radicals [12–14]. This work is focused on spectral changes of phenol, 2-chlorophenol (2CPH), 2-aminophenol (2APH), and 2-nitrophenol (2NPH) in polar protic and aprotic solvents.

The substituent effect on the O-H bond dissociation energy (BDE) of phenols has been shown to depend on factors such as inductive or electrostatic effect, resonance effect, and hydrogen-bonding interactions in the respective solvents [15]. Using the Hammett-type parameters σ_P^+ and R^+ to investigate a series of parasubstituted phenols, Zhang et al. [16] found that resonance effect contributed largely to the O-H BDE. This effect was high in electron withdrawing groups as compared to electron-donating analogs. For example, although chlorine is an electron-withdrawing group, it showed an electron-donating resonance effect because of delocalization of nonbonding electrons. According to Guerra et al. [15], electron-donating substituents lead to a better stabilization of phenoxyl radicals in water whereas electron-withdrawing groups preferentially stabilize the parent phenol. This suggests that the stabilization of phenols in solution cannot solely be attributed to the effect of substituents but a synergy between contributions from both substituents and the solvent.

Analyses of the UV spectra of *ortho*-substituted phenols is generally difficult [3] because several factors such as electrostatic effects of the substituent, resonance effects, inter- and intramolecular hydrogen-bonding interactions,

and steric effects have been found to contribute. Korth et al. [17] have shown by means of thermodynamic and kinetic methods that, in a nonhydrogen bonding solvent, 2-methoxyphenol exists entirely in a hydrogen bonding form, whereas there is a strong interaction with hydrogen bond acceptor solvents to create a bifurcated complex which shifts the absorption maximum bathochromically. Because of their importance as model systems for hydrogen-bonding interactions and solvent-solute interactions and in photoinduced intercluster proton-transfer processes, these interactions have been investigated by various *ab initio* and density functional theory methods [2, 16]. In this paper, we present a comprehensive study of the effect of the chloro, amino, and nitro *ortho*-substituents on the solvatochromism of phenol in methanol and dimethyl sulfoxide (DMSO). These solvents are among the most important polar protic (methanol) and aprotic (DMSO) solvents used in organic and coordination chemistry. Although dimethyl sulfoxide and dimethyl sulfone (DMSO2) are classified as aprotic solvents, Clark et al. [18] have shown by B3PW91 and MP2-FC computational studies that the significant success of these solvents in dissolving most solutes can be attributed to sufficiently strong σ-holes on the sulfur atom which interacts electrostatically with nucleophilic regions of other molecules. These interactions are also effective when π-electrons are involved. It has been demonstrated computationally that polar protic solvents such as methanol interact with solutes such as phenols by accepting and donating hydrogen bonds. These interactions, according to Guerra et al., have little effect on the bond dissociation energy (BDE) of phenol [15]. According to them, significant contributors to the BDE are the type and position of substituents [15].

Our interest in the UV absorption spectra of *o*-substituted phenols lies in the fact that the proximity of the substituent makes it possible to form intramolecular interactions with the phenol OH group, and it can also form intermolecular hydrogen bonds with the solvent as well as engage in bifurcate interactions. The electron-accepting and electron-donating abilities of the substituent also increase or decrease the electron density on the phenyl ring. These are important factors that influence the free radical scavenging activities and solvatochromism of substituted phenols. The geometry and electronic effect of the substituents have been analysed by natural bond orbital (NBO) analysis. Natural population analysis (NPA) and Frontier molecular orbitals (FMOs) have also been used to assess the resonance contribution of the substituents to the electronic structure of the phenols. Furthermore, full interaction maps of the compounds have been assessed using the *Mercury* program to identify possible spots for inter-and intramolecular hydrogen and halogen bonding since these interactions affect the spectral properties of phenols.

2. Experimental Details

All the phenols and solvents used for this work were purchased from VWR Chemicals, UK, and used without further purification. The phenols were completely soluble in methanol and DMSO. Stock solutions of 2 mM concentrations were prepared for all the compounds. These were further diluted to working concentrations between 0.2 and 1.0 mM. UV absorption spectra were then taken on a Spectroquant UV/VIS spectrophotometer Pharo 300 at the Chemistry Laboratory of the Institute of Industrial Research, Council for Scientific and Industrial Research, Ghana, between 250 and 400 nm. Molar absorptivities (ε) were also estimated by measuring the absorbance of the diluted solutions at the respective λ_{max} values.

3. CSD Analysis

Analyses of the full interaction maps of the phenols were performed using version 5.38 of the Cambridge Structural Database (CSD) (November 2016) plus one update [19]. Version 1.19 of the CSD program *ConQuest* was used to perform substructure searches of phenol, 2CPH, 2APH, and 2NPH. The following secondary search criteria were employed: 3D coordinates determined; crystallographic R factor $\leq$ 0.05; no disorder in the crystal structure; no bonding; no ions; and no powder structures and only organic structures (according to the standard CSD definitions). Structures with monomeric units were selected for this work. The search revealed fifteen (15) crystal structures bearing the phenol moiety, one 2CPH, and four (4) structures bearing 2APH. Crystals structures with the following reference codes were then chosen: PHENOL03 [20] with $z' = 3$, WANMUU [21], $z' = 3$, and AMPHOM02 [22] with $z' = 1$. There was, however, no crystal structure of 2NPH in the CSD as at the time of preparing this manuscript. The structures were visualized using version 3.9 of the CSD program *Mercury*. Probes such as uncharged NH nitrogen, alcohol oxygen, oxygen atom, aromatic CH carbon, and C-Cl chlorine were used as proxies to provide interaction maps which indicate positions of hydrogen bond acceptors (shown in red), donors (blue), and any possibility of halogen bonding (shown in green) [19].

4. Computational Details

All the input files of the respective phenols were prepared using the GausView 5.0.8 molecular viewer [19]. Full unconstrained geometry optimizations were carried out at the density functional theory (DFT) using Becke's three-parameter hybrid method and the Lee–Yang–Parr correlation functional (B3LYP) with the 6-31++G(d,p) basis set [23]. The Gaussian 09 program [24] was used for all computations. The optimized geometries are shown in Figure 1. The structures were characterized as minima (no imaginary frequency) in their potential energies through vibrational frequency analyses [25]. The gas-phase UV spectra were analyzed using the time-dependent density functional theory (TD-DFT) method on the optimized geometries. TD-DFT is a very effective technique for excited state calculations and has been used successfully to study phenols of increasing size [2]. The effect of the substituents on the electron distribution in the phenols was investigated using

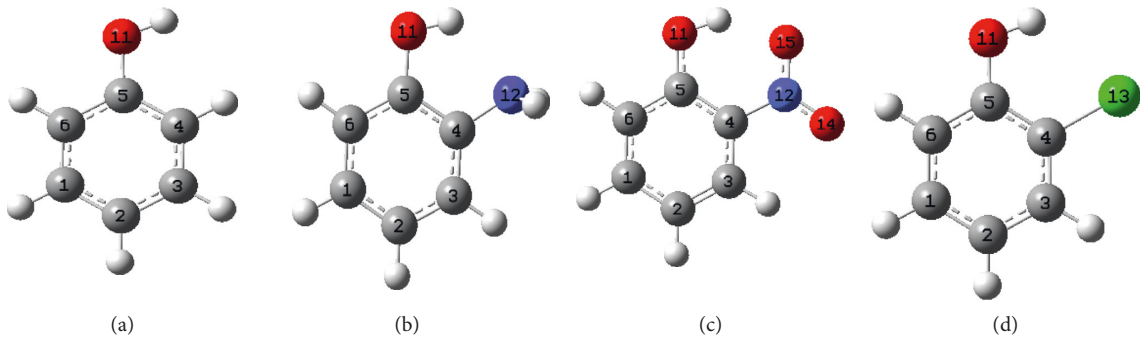

(a) (b) (c) (d)

Figure 1: Molecular geometries of the phenols: (a) phenol; (b) 2-aminophenol; (c) 2-nitrophenol; (d) 2-cholophenol.

natural bond orbital (NBO) and natural population analysis (NPA). The net atomic charge and Frontier molecular orbitals (FMOs) were also performed at the same level of theory.

5. Results and Discussion

Figures 2–5 show the spectra of the phenols in methanol and DMSO, respectively. From Figure 2, the absorption maximum (λ_{max}) of phenol is 272 nm in methanol and 277 nm in DMSO, a bathochromic shift of 5 nm. This π-π^* excitation is relatively more stable in DMSO than in methanol. As shown in Table 1, the intensities of these bands are relatively high (ε = 2344 in methanol and 14454 in DMSO). Similar shift and molar absorptivities were observed for 2CPH (Figure 3). The presence of the chloro-substituent, however, increased the bathochromism of the λ_{max} of phenol by 5 nm in methanol and 2 nm in DMSO. TD-DFT evaluation in Table 2 shows similar shifts in λ_{max} with 2NPH recording the highest. According to Krivoruchka et al. [26], 2-nitrophenol forms inter-, intra-, and bifurcate hydrogen bonds which accounts for the shifts in its OH stretching absorption to lower frequencies. Similar bonding modes could account for the relatively high bathochromism of 2NPH observed computationally.

Using the inductive effect interpretation, the electron-withdrawing tendency of the Cl substituent has the potential of reducing the electron density of the phenyl ring and shifting the λ_{max} hypsochromically relative to the parent phenol. This negative inductive effect has been reported to increase the acidity of various substituted phenols [3]. The reverse was, however, observed. This can be attributed to the delocalization of nonbonding Cl electrons onto the phenyl π system, thereby increasing the electron density and shifting λ_{max} in the observed direction [3]. The stronger π-π^* stacking of 2APH with increasing concentration in both solvents is shown in Figure 4.

From Figure 5, the λ_{max} of 2NPH shows the highest bathochromic shift relative to the parent phenol despite the fact that the nitro group (a ring deactivating group) is expected to shift the λ_{max} to shorter wavelength. According to the resonance theory, the π-electrons on the O14 and O15 atoms can be delocalized into π^* molecular orbitals on the phenyl ring and cause a bathochromic shift in λ_{max} as observed [27].

In order to better reconcile the observed absorption spectra and the electronic properties of the phenols, we performed NBO and second-order perturbation theory analysis of Fock matrix [18, 25]. These provide details about the type of hybridization, electron distribution, nature and strength of bonding, and the charge distribution on the respective atoms [28]. In Table 3, the bond lengths show significant substituent effect. Generally, most of the optimized bond lengths are slightly greater than the experimental values due to the fact that the theoretical calculations were performed on a single molecule in the gas phase with no intermolecular interactions, whereas the experimental data belong to molecules in crystal structures with substantial interactions under different lattice parameters. Relatively, the bond lengths are shorter in 2CPH as compared to phenol except the C4-C5 and C5-C6 bonds which were longer. This is because the electronegative Cl substituent withdraws the σ-shared pair of electrons onto itself making C4 slightly positive. This electron pull runs through the C4-C5 bond and decreases its electron density. The combined electronegativities of Cl and O11 contribute to the reduction in the electron density in the C4-C5 and C5-C6 bonds, thereby increasing their lengths [29].

Generally, the presence of the o-substituent increased the lengths of the C4-C5 and O11-H12 bonds in the order Cl < NH_2 < NO_2. This correlates strongly with the negative inductive effect of the substituent [17] which contributes to withdrawing σ-shared pair of electrons from the phenyl ring. These results are also in agreement with the pKa values of these substituted phenols [1, 4]. According to Guerra et al. [15], polar protic solvents such as methanol are better at stabilizing the phenolic OH group because they act as hydrogen bond acceptor (HBA) as well as hydrogen bond donor (HBD) groups in which the methanol oxygen acts as both an acceptor and donor. Therefore, the higher the acidity of the phenol, the higher its stability in methanol. This could explain the slightly higher bathochromic shifts of 2NPH and 2APH in methanol relative to DMSO. In DMSO, the noncovalent interactions are between the DMSO-S and the phenol-O. According to Clark et al., the significant positive σ-hole on the sulfur atom of DMSO interacts electrostatically with negative regions of Lewis bases such as the lone pairs of electrons on the oxygen atom of phenol. Because these σ-hole interactions are weaker than conventional

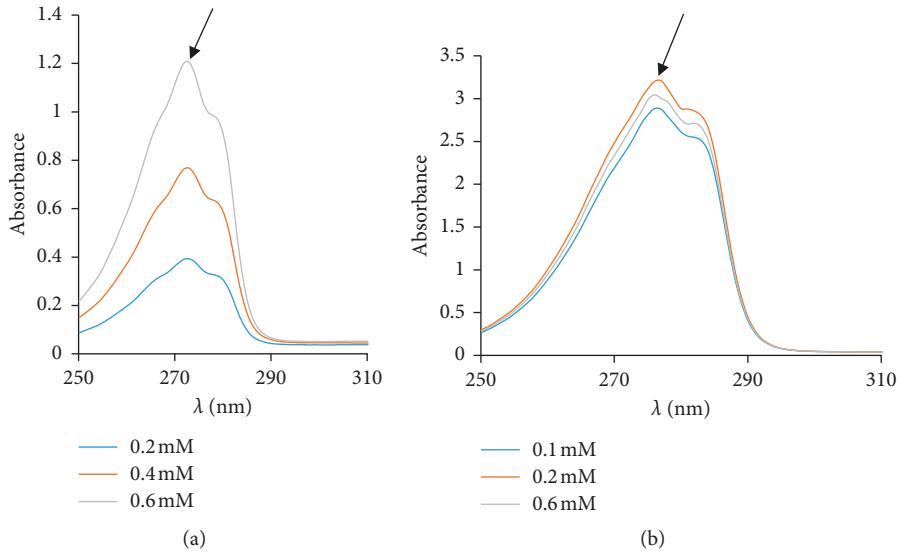

Figure 2: UV absorption spectra of phenol in (a) methanol, and (b) DMSO with arrows indicating the λ_{max}.

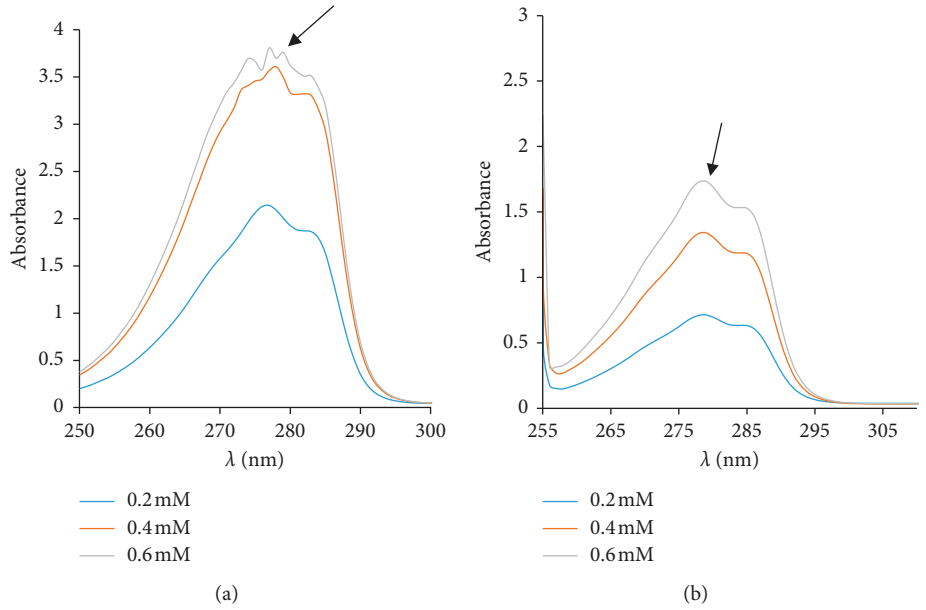

Figure 3: UV absorption spectra of 2-chlorophenol in (a) methanol and (b) DMSO with arrows indicating the λ_{max}.

hydrogen bonds, relatively acidic phenols seem to be more stable in methanol than DMSO.

To further understand the effect of the *o*-substituents on the electron distribution in the phenol molecule, we performed NBO analyses on the respective molecules. From Table 4, there is considerable shifting of shared σ-bonding electrons towards C4 (*ortho* carbon).

This delocalization is greatest in 2NPH where the percentage electron distribution between C3 and C4 is 48.3% and 51.7%, respectively, followed by 2CPH, 48.5%–51.5% and 2APH (49.1%–50.9%). This is due to the negative inductive effect of the respective substituents which leads to the withdrawal of electrons from the σ-framework of the phenyl ring. This inductive effect is similarly transmitted through the C4-C5 σ-bond with C4 having the highest percentage of electrons in all the compounds. These observations further explain the weakening of the C3-C4 and C4-C5 bonds as observed in Table 3.

Table 4 also shows the distribution of the various π-electrons in the respective structures. There is 60% delocalization of shared (C4-C5) electrons towards C4. This electron pull can be attributed to the greater electron withdrawing ability of the O14 (60.1%) in the N12-O14 π-bond as shown in Figure 6. This electron pull increases the π-electron conjugation of the phenol ring, thereby causing a bathochromic shift in λ_{max} as observed in Figure 5. It can also be seen that the π-electron density of the C1-C6 bond is

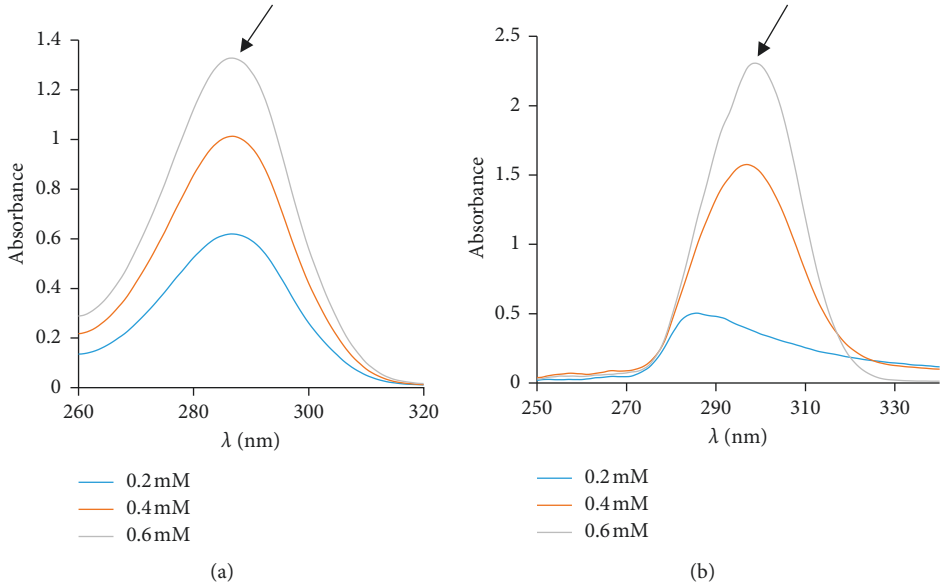

Figure 4: UV absorption spectra of 2-aminophenol in (a) methanol and (b) DMSO with arrows indicating the λ_{max}.

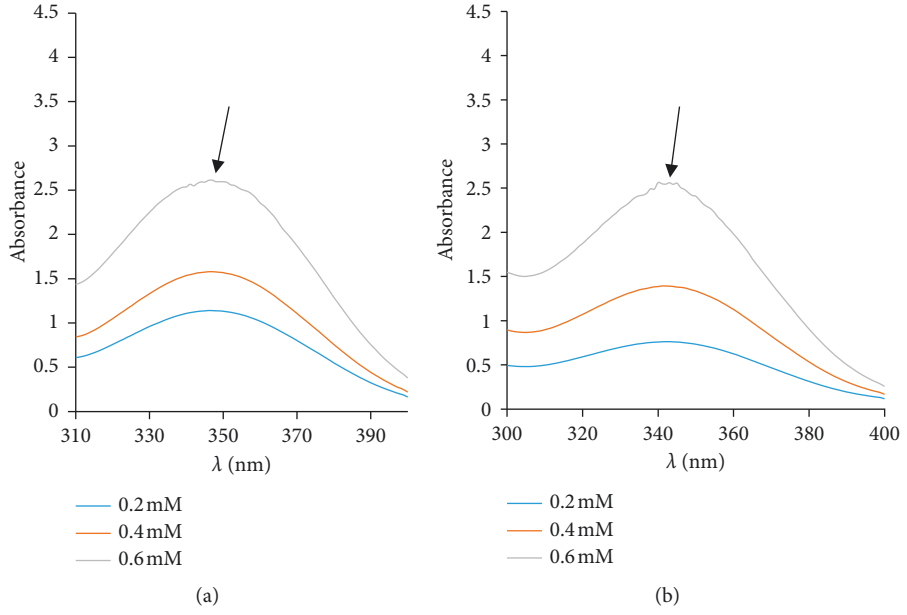

Figure 5: UV absorption spectra of 2-nitrophenol in (a) methanol and (b) DMSO with arrows indicating the λ_{max}.

Table 1: Experimentally determined wavelength of maximum absorption (λ_{max}) and molar absorptivity (ε) of the phenols.

Solvent	λ_{max} (ε)			
	Phenol	2CPH	2APH	2NPH
Methanol	272 (2344)	277 (3467)	287 (3090)	347 (2951)
Dimethyl sulfoxide	277 (14454)	279 (14454)	285 (2951)	343 (5623)

fairly constant (1.696) and not affected by the resonance effect of the substituents.

However, electron density of the C2-C3 π-bond increased in the order Cl < NH_2 < NO_2 as a result of the proximity to the substituents which caused substantial π-electron delocalization into the C2-C3 bond. These interactions increase the electron density on the phenyl ring and contribute to the π-π^* interactions [2, 30] which shift the λ_{max} to longer wavelengths.

Table 5 shows results of the second-order perturbation of the Fock matrix. These show the donor-acceptor interactions which contribute to increasing the electron density on the

Table 2: TD-DFT calculated λ_{max} and ε of the optimized structures.

Compound	λ_{max}	ε
Phenol	246	1400
2CPH	249	1800
2APH	254	2500
2NPH	362	2480

Table 3: Experimental and calculated lengths (Å) of some selected bonds in the studied compounds.

Bond	Length							
	Phenol		2CPH		2APH		2NPH	
	Exptal	Calc	Exptal	Calc	Exptal	Calc	Exptal	Calc
C1-C2	1.380	1.3996	1.386	1.3993	1.379	1.3999	1.373	1.4078
C1-C6	1.389	1.3947	1.393	1.3930	1.378	1.3949	1.354	1.3861
C2-C3	1.395	1.3966	1.390	1.3954	1.379	1.3976	1.365	1.3835
C3-C4	1.381	1.3979	1.384	1.3939	1.382	1.3973	1.393	1.4059
C4-C5	1.397	1.3992	1.392	1.4030	1.397	1.4081	1.396	1.4186
C5-C6	1.394	1.3993	1.390	1.4003	1.377	1.3989	1.384	1.4071
O11-H12		0.9661		0.9698		0.9783		0.9865

Table 4: NBO population analyses for the respective compounds.

Bond	Type	Phenol		2-Chlorophenol		2-Aminophenol		2-Nitrophenol	
		ED	Occupancy	ED	Occupancy	ED	Occupancy	ED	Occupancy
C1-C2	$\sum$	1.982	50.2% C1-49.8% C2	1.982	50% C1-50% C2	1.981	50% C1-50% C2	1.982	50.1% C1-49.9% C2
C1-C6	$\sum$	1.978	49.7% C1-50.3% C6	1.978	49.6% C1-50.4% C6	1.977	49.7% C1-50.3% C6	1.980	49.7% C1-50.3% C6
C1-C6	π	1.696	47.8% C1-52.2% C6	1.696	48.2% C1-51.8% C6	1.696	47.9% C1-52.1% C6	1.698	46.4% C1-53.6% C6
C2-C3	σ	1.981	49.7% C2-50.3% C3	1.972	49.2% C2-50.8% C3	1.978	49.4% C2-50.6% C3	1.978	49.3% C2-50.7% C3
C2-C3	π	1.680	51.9% C2-48.1% C3	1.686	51.4% C2-48.6% C3	1.690	51.5% C2-58.5% C3	1.702	53% C2-47% C3
C3-C4	σ	1.977	49.4% C3-50.6% C4	1.980	48.5% C3-51.5% C4	1.979	49.1% C3-50.9% C4	1.974	48.3% C3-51.7% C4
C4-C5	σ	1.981	49.6% C4-50.4% C5	1.980	50.6% C4-49.4% C5	1.975	50.2% C4-49.8% C5	1.978	51% C4-49% C5
C4-C5	π	1.659	54.2% C4-45.8% C5	1.673	56.7% C4-43.3% C5	1.636	55.1% C4-44.9% C5	1.612	60% C4-40% C5
C5-C6	σ	1.976	50.7% C5-49.3% C6	1.970	51.2% C5-48.8% C6	1.976	50.9% C5-49.1% C6	1.976	51.2% C5-48.8% C6
C5-O11	σ	1.995	33.3% C5-66.7% O11	1.995	33.9% C5-66.1% O11	1.995	33.8% C5-66.2% O11	1.994	34.4% C5-65.6% O11
C4-Cl13	σ			1.989	45% C4-55% Cl13				
C4-N12	σ					1.990	40.8% C4-59.2% N2		
C4-N14	σ							1.989	37.3% C4-62.7% N14
N12-O14	σ							1.996	49.1% N12-50.9% O14
	π							1.988	39.9% N12-60.1% O14
N12-O15	σ							1.995	49% N12-50.1% O15
LP (1)O11		1.979	100% O11	1.978	100% O11	1.979	100% O11	1.973	100% O11
LP (2)O11		1.881	100% O11	1.867	100% O11	1.860	100% O11	1.807	100% O11
LP (1)Cl13				1.994	100% O11				
LP (2)Cl13				1.959	100% O11				
LP (3)Cl13				1.943	100% O11				
LP (1)O14								1.982	100% O14
LP (2)O14								1.890	100% O14
LP (1)O15								1.975	100% O15
LP (2)O15								1.898	100% O15
LP (3)O15								1.530	100% O15

phenyl ring in the excited state [31]. The strongest π-π^* interaction is between LP(3) on O15 and N12-O14 of 2NPH with interaction energy of 123.96 kJ/mol followed by LP(2) on O11 to the π^* molecular orbital of C4-C5, 40.37 kJ/mol and C4-C5 to N12-O14 π^*s orbitals of 37.97 kJ/mol.

These substantial delocalization of π electrons into π^* molecular orbitals also increases the stability of the excited state which contributes to π-π^* interactions as observed in polar solvents [32]. The effects of the inductive and resonance effects on the charge density of the respective atoms are shown in Table 6. Phenol, an *ortho*/*para* director to nucleophilic substitution, has higher electron densities on C4, C2, and C6 as shown in Table 6.

Specifically, the electron density on C4 is reduced as a result of the negative inductive effect of the substituents. This effect is severe in 2APH because the nitro and chloro

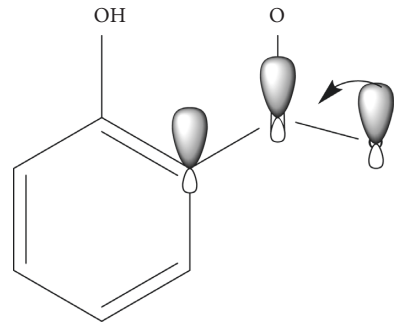

Figure 6: Resonance structure of 2NPH.

Table 5: Second-order perturbation theory analysis of Fock matrix in NBO basis for the respective phenols.

Donor	Type	Acceptor	Type	E (2) (kJ/mol)			
				Phenol	2-Chlorophenol	2-Aminophenol	2-Nitrophenol
C1-C6	π	C2-C3	π^*	17.27	17.84	17.42	15.18
	π	C4-C5	π^*	22.67	23.58	22.69	24.68
C2-C3	π	C4-C5	π^*	17.39	17.81	17.56	15.53
	π	C1-C6	π^*	21.93	21.04	21.19	21.72
C4-C5	π	C2-C3	π^*	22.33	21.30	25.50	21.32
	π	C1-C6	π^*	16.46	15.10	16.47	12.15
C4-C5	π	N12-O14	π^*				37.97
O11	LP (2)	C4-C5	π^*	27.42	31.64	31.33	40.37
	LP (1)	C4-C5	π^*	6.43	6.06	5.83	8.05
Cl13	LP (1)	C3-C4	σ^*		1.36		
	LP (2)	C3-C4	σ^*		3.78		
N12	LP (1)	C3-C4	σ^*			8.79	
		C4-C5	σ^*			3.86	
O15	LP (3)	N12-O14	π^*				123.96

Table 6: Natural charge (atomic units) of some selected atoms in the compounds.

Atom	Charge			
	Phenol	2-Chlorophenol	2-Aminophenol	2-Nitrophenol
C1	−0.2177	−0.2199	−0.2197	−0.1792
C2	−0.2864	−0.2542	−0.2678	−0.2619
C3	−0.2180	−0.2331	−0.2362	−0.1939
C4	−0.3160	−0.1215	0.0422	−0.0142
C5	0.3076	0.2968	0.3140	0.3549
C6	−0.2861	−0.2698	−0.2836	−0.2806
O11	−0.7038	−0.6996	−0.7093	−0.6772
Cl13		−0.0110		
N12			−0.9342	0.4949
O14				−0.3630
O15				−0.4395

groups have nonbonding and π-electrons which can be delocalized into antibonding and Rydberg orbitals to decrease the net effect of polarization of the C4-substituent bond [3]. As shown, the N12 of 2APH has the highest electron density of −0.9342 because of the localization of its nonbonding electrons.

Figure 7 shows the effect of *o*-substitution on the energy of the Frontier orbitals. The smaller the HOMO-LUMO gap, the higher the bathochromic shift. The values range from −5.823 eV for phenol to −3.973 eV for 2-nitrophenol. The lowest Frontier orbital gap for 2NPH confirms the extension of the π-electron density of the phenyl ring onto the NO_2, thereby increasing its conjugation and causing a red shift in its absorption spectra. Finally, we report the full interaction maps of the compounds. Generally, the hydrophobic propensity regions above and below the phenyl rings remain unchanged as shown in Figure 8. The interaction maps around 2APH show hydrogen bond donor (shown in blue) and acceptor (shown in red) regions around the NH_2 and a strong acceptor region on the OH group.

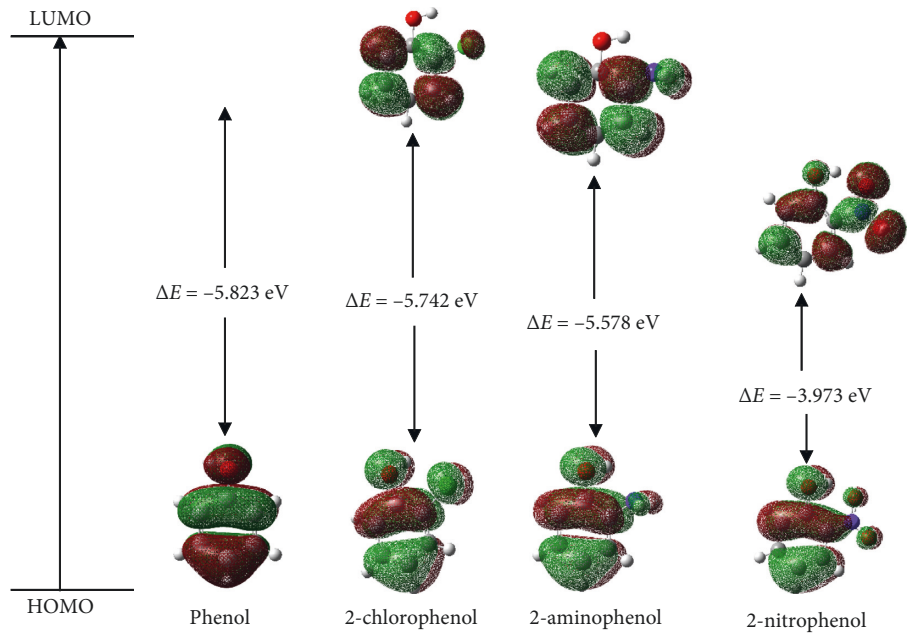

Figure 7: Frontier molecular orbitals of the phenols.

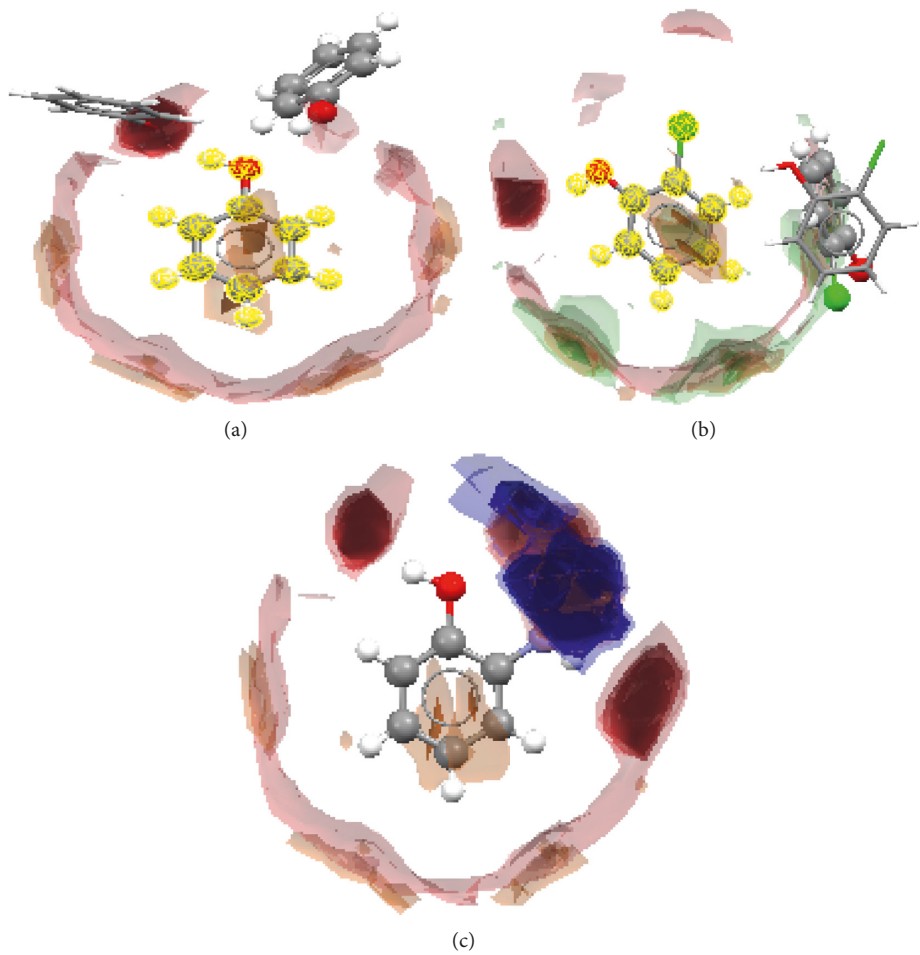

Figure 8: Full interaction maps of (a) phenol, (b) 2CPH, and (c) 2APH.

These regions are potential sites for interactions between 2APH and both polar protic and aprotic solvents such as methanol and DMSO which act as both hydrogen bond acceptors and donors. The interaction maps around phenol and 2CPH do not differ that much except for the propensity for halogen bonding (shown in green) which was observed in 2CPH. Generally, investigation of the full interaction maps show that 2APH has the highest propensity for inter- and intramolecular interaction as compared to phenol and 2CPH. This supports the data reported in Table 1 where λ_{max} of 2APH shows the highest bathochromic shift compared to phenol and 2CPH.

6. Conclusion

Ortho-substituted phenols have the ability to engage in intra- and intermolecular bonding as well as bifurcate interactions involving solvent molecules. These interactions significantly alter the spectroscopic behavior of these phenols. The electron-withdrawing and electron-donating abilities of these substituents also affect the π-system of phenols and influence their spectral characteristics in different solvents. In this work, we have shown by NBO and NPA analyses that, although Cl, an electron-withdrawing group, decreases the electron density on phenol by negative inductive effect, it also delocalizes nonbonding electrons onto the phenyl ring by resonance, thereby increasing its electron density. The net effect is the red shift of the UV spectra of 2-chlorophenol in methanol and dimethyl sulfoxide. Similar solvatochromism was also observed in 2-nitrophenol. Full interaction maps of phenol, 2CPH, and 2APH have been accessed using the *Mercury* program of the CSD. It shows hydrogen bond donor and acceptor regions around the NH_2 and a strong acceptor region on the OH group of 2NPH. 2CPH also exhibits propensity for halogen bonding which explains the observed UV spectra.

Data Availability

The data used to support the findings of this study are available from the corresponding author upon request.

Conflicts of Interest

The authors declare that there are no conflicts of interest regarding the preparation and publication of this manuscript.

Acknowledgments

The authors are thankful to the Cambridge Crystallographic Data Center (CCDC) for the opportunity to use the Cambridge Structural Database (CSD) for the molecular searches and full interaction map (FIM) studies.

References

[1] M. D. Liptak, K. C. Gross, P. G. Seybold, S. Feldgus, and G. C. Shields, "Absolute pKa determinations for substituted phenols," *Journal of the American Chemical Society*, vol. 124, no. 22, pp. 6421–6427, 2002.

[2] L. Zhang, G. H. Peslherbe, and H. M. Muchall, "Ultraviolet absorption spectra of substituted phenols: a computational study," *Photochemistry and Photobiology*, vol. 82, no. 1, pp. 324–331, 2006.

[3] D.-S. Ahn, S.-W. Park, S. Lee, and B. Kim, "Effects of substituting group on the hydrogen bonding in phenol–H_2O complexes: ab initio study," *Journal of Physical Chemistry A*, vol. 107, no. 1, pp. 131–139, 2003.

[4] K. C. Gross and P. G. Seybold, "Substituent effects on the physical properties and pKa of phenol," *International Journal of Quantum Chemistry*, vol. 85, no. 4-5, pp. 569–579, 2001.

[5] K. Roy and P. L. Popelier, "Predictive QSPR modeling of the acidic dissociation constant (pKa) of phenols in different solvents," *Journal of Physical Organic Chemistry*, vol. 22, no. 3, pp. 186–196, 2009.

[6] M. Schmitt, M. Böhm, C. Ratzer et al., "Determining the intermolecular structure in the S0 and S1 states of the phenol dimer by rotationally resolved electronic spectroscopy," *ChemPhysChem*, vol. 7, no. 6, pp. 1241–1249, 2006.

[7] R. C. Barreto, K. Coutinho, H. C. Georg, and S. Canuto, "Combined Monte Carlo and quantum mechanics study of the solvatochromism of phenol in water. The origin of the blue shift of the lowest π–π∗ transition," *Physical Chemistry Chemical Physics*, vol. 11, no. 9, pp. 1388–1396, 2009.

[8] A. Zilly, C. Souza, I. Barbosa-Tessmann, and R. Peralta, "Decolorization of industrial dyes by a Brazilian strain of Pleurotus pulmonarius producing laccase as the sole phenol-oxidizing enzyme," *Folia Microbiologica*, vol. 47, no. 3, pp. 273–277, 2002.

[9] J. Sargolzaei, A. Hedayati Moghaddam, A. Nouri, and J. Shayegan, "Modeling the removal of phenol dyes using a photocatalytic reactor with SnO_2/Fe_3O_4 nanoparticles by intelligent system," *Journal of Dispersion Science and Technology*, vol. 36, no. 4, pp. 540–548, 2015.

[10] I. Goldberg, A. Sasson, A. Gat, A. Srebrnik, and S. Brenner, "Pemphigus vulgaris triggered by glibenclamide and cilazapril," *Acta Dermatovenerologica Croatica*, vol. 13, no. 3, pp. 153–155, 2005.

[11] S. Oliver, B. Gillespie, M. Lewis et al., "Efficacy of a new premilking teat disinfectant containing a phenolic combination for the prevention of mastitis," *Journal of Dairy Science*, vol. 84, no. 6, pp. 1545–1549, 2001.

[12] Z. Maksimović, Đ. Malenčić, and N. Kovačević, "Polyphenol contents and antioxidant activity of Maydis stigma extracts," *Bioresource Technology*, vol. 96, no. 8, pp. 873–877, 2005.

[13] Y. Kiselova, D. Ivanova, T. Chervenkov, D. Gerova, B. Galunska, and T. Yankova, "Correlation between the in vitro antioxidant activity and polyphenol content of aqueous extracts from Bulgarian herbs," *Phytotherapy Research*, vol. 20, no. 11, pp. 961–965, 2006.

[14] M. H. Gordon, F. Paiva-Martins, and M. Almeida, "Antioxidant activity of hydroxytyrosol acetate compared with that of other olive oil polyphenols," *Journal of Agricultural and Food Chemistry*, vol. 49, no. 5, pp. 2480–2485, 2001.

[15] M. Guerra, R. Amorati, and G. F. Pedulli, "Water effect on the O–H dissociation enthalpy of para-substituted phenols: a DFT study," *Journal of Organic Chemistry*, vol. 69, no. 16, pp. 5460–5467, 2004.

[16] H. Y. Zhang, Y. M. Sun, and X. L. Wang, "Substituent effects on O-H bond dissociation enthalpies and ionization potentials of catechols: a DFT study and its implications in the rational design of phenolic antioxidants and elucidation of structure–activity relationships for flavonoid antioxidants,"

Chemistry-A European Journal, vol. 9, no. 2, pp. 502–508, 2003.

[17] H.-G. Korth, M. I. De Heer, and P. Mulder, "A DFT study on intramolecular hydrogen bonding in 2-substituted phenols: conformations, enthalpies, and correlation with solute parameters," *Journal of Physical Chemistry A*, vol. 106, no. 37, pp. 8779–8789, 2002.

[18] T. Clark, J. S. Murray, P. Lane, and P. Politzer, "Why are dimethyl sulfoxide and dimethyl sulfone such good solvents?," *Journal of Molecular Modeling*, vol. 14, no. 8, pp. 689–697, 2008.

[19] S. Tetteh and R. Zugle, "Theoretical study of terminal vanadium(V) chalcogenido complexes bearing chlorido and methoxido ligands," *Journal of Chemistry*, vol. 2017, Article ID 6796321, 8 pages, 2017.

[20] V. Zavodnik, V. Bel'skii, and P. Zorkii, "Crystal structure of phenol at 123oK," *Journal of Structural Chemistry*, vol. 28, no. 5, pp. 793–795, 1988.

[21] I. D. Oswald, D. R. Allan, G. M. Day, W. S. Motherwell, and S. Parsons, "Realizing predicted crystal structures at extreme conditions: the low-temperature and high-pressure crystal structures of 2-chlorophenol and 4-fluorophenol," *Crystal Growth & Design*, vol. 5, no. 3, pp. 1055–1071, 2005.

[22] B. Babu, J. Chandrasekaran, and S. Balaprabhakaran, "Growth, structural, spectral, optical and electrical properties of 2-aminophenol single crystals," *Optik-International Journal for Light and Electron Optics*, vol. 125, no. 13, pp. 3005–3008, 2014.

[23] Z. Chen, L. Wang, G. Zou, X. Cao, Y. Wu, and P. Hu, "A retrievable and highly selective fluorescent probe for monitoring dihydrogen phosphate ions based on a naphthalimide framework," *Spectrochimica Acta Part A: Molecular and Biomolecular Spectroscopy*, vol. 114, pp. 323–329, 2013.

[24] M. Frisch, G. Trucks, H. Schlegel et al., *Gaussian 09, Revision A. 1 [Computer Software]*, Gaussian, Wallingford, CT, USA, 2009.

[25] A. M. Mansour, "Coordination behavior of sulfamethazine drug towards Ru (III) and Pt (II) ions: synthesis, spectral, DFT, magnetic, electrochemical and biological activity studies," *Inorganica Chimica Acta*, vol. 394, pp. 436–445, 2013.

[26] I. Krivoruchka, A. Vokin, T. Aksamentova et al., "Solvatochromism of heteroaromatic compounds: XXII. Effect of bifurcate hydrogen bond on the IR spectrum and dipole moment of N-(4-methyl-2-nitrophenyl) acetamide in solution," *Russian Journal of General Chemistry*, vol. 74, no. 1, pp. 120–127, 2004.

[27] T. M. Krygowski and B. T. Stępień, "Sigma-and pi-electron delocalization: focus on substituent effects," *Chemical Reviews*, vol. 105, no. 10, pp. 3482–3512, 2005.

[28] B. Shainyan, N. Chipanina, T. Aksamentova, L. Oznobikhina, G. Rosentsveig, and I. Rosentsveig, "Intramolecular hydrogen bonds in the sulfonamide derivatives of oxamide, dithiooxamide, and biuret. FT-IR and DFT study, AIM and NBO analysis," *Tetrahedron*, vol. 66, no. 44, pp. 8551–8556, 2010.

[29] A. R. Campanelli, A. Domenicano, and F. Ramondo, "Electronegativity, resonance, and steric effects and the structure of monosubstituted benzene rings: an ab initio MO study," *Journal of Physical Chemistry A*, vol. 107, no. 33, pp. 6429–6440, 2003.

[30] J. B. Barbour and J. M. Karty, "Resonance and field/inductive substituent effects on the gas-phase acidities of para-substituted phenols: a direct approach employing density functional theory," *Journal of Physical Organic Chemistry*, vol. 18, no. 3, pp. 210–216, 2005.

[31] B. Kosar and C. Albayrak, "Spectroscopic investigations and quantum chemical computational study of (E)-4-methoxy-2-[(p-tolylimino) methyl] phenol," *Spectrochimica Acta Part A: Molecular and Biomolecular Spectroscopy*, vol. 78, no. 1, pp. 160–167, 2011.

[32] M. Wielgus, J. Michalska, M. Samoc, and W. Bartkowiak, "Two-photon solvatochromism III: experimental study of the solvent effects on two-photon absorption spectrum of p-nitroaniline," *Dyes and Pigments*, vol. 113, pp. 426–434, 2015.